

# Metallomics

## Accepted Manuscript



This is an *Accepted Manuscript*, which has been through the RSC Publishing peer review process and has been accepted for publication.

*Accepted Manuscripts* are published online shortly after acceptance, which is prior to technical editing, formatting and proof reading. This free service from RSC Publishing allows authors to make their results available to the community, in citable form, before publication of the edited article. This *Accepted Manuscript* will be replaced by the edited and formatted *Advance Article* as soon as this is available.

To cite this manuscript please use its permanent Digital Object Identifier (DOI®), which is identical for all formats of publication.

More information about *Accepted Manuscripts* can be found in the [Information for Authors](#).

Please note that technical editing may introduce minor changes to the text and/or graphics contained in the manuscript submitted by the author(s) which may alter content, and that the standard [Terms & Conditions](#) and the [ethical guidelines](#) that apply to the journal are still applicable. In no event shall the RSC be held responsible for any errors or omissions in these *Accepted Manuscript* manuscripts or any consequences arising from the use of any information contained in them.

# Altered transition metal homeostasis in Niemann-Pick disease, Type C1

Ya Hui Hung<sup>a</sup>, Noel G. Faux<sup>a</sup>, David W. Killilea<sup>b</sup>, Nicole Yanjanin<sup>c</sup>, Sally Firnkes<sup>d</sup>,  
Irene Volitakis<sup>a</sup>, George Ganio<sup>a</sup>, Mark Walterfang<sup>e</sup>, Caroline Hastings<sup>f</sup>, Forbes D. Porter<sup>c</sup>, Daniel  
S. Ory<sup>d</sup>, and Ashley I. Bush<sup>a</sup>

- a. Oxidation Biology Unit, The Florey Institute of Neuroscience and Mental Health, The University of Melbourne, Parkville, Victoria, 3010, Australia
- b. Nutrition & Metabolism Center, Children's Hospital Oakland Research Institute, Oakland, CA 94609, USA
- c. Program in Developmental Endocrinology and Genetics, Eunice Kennedy Shriver National Institute of Child Health and Human Development, National Institute of Health, Department of Health and Human Services, Bethesda, MD 20892, USA
- d. Diabetic Cardiovascular Disease Center, Washington University School of Medicine, St. Louis, MO 63110, USA
- e. Neuropsychiatry Unit, Royal Melbourne Hospital and Melbourne Neuropsychiatry Centre, Melbourne, Victoria, 3050, Australia
- f. Children's Hospital & Research Center Oakland, CA 94609, USA

Correspondence to:

Professor Ashley I. Bush

Oxidation Biology Unit,

The Florey Institute of Neuroscience and Mental Health,

Level 4, Kenneth Myer Building

The University of Melbourne

Parkville, Victoria, 3010,

Australia.

Tel. +61 3 9035 6532

E-mail: [ashley.bush@florey.edu.au](mailto:ashley.bush@florey.edu.au)

**ABSTRACT**

The loss of NPC1 protein function is the predominant cause of Niemann-Pick type C1 disease (NP-C1), a systemic and neurodegenerative disorder characterized by late-endosomal/lysosomal accumulation of cholesterol and other lipids. Limited evidence from post-mortem human tissues, an *Npc1*<sup>-/-</sup> mouse model, and cell culture studies also suggest failure of metal homeostasis in NP-C1. To investigate these findings, we performed a comprehensive transition metal analysis of cerebrospinal fluid (CSF), plasma and tissue samples from human NP-C1 patients and an *Npc1*<sup>-/-</sup> mouse model. NPC1 deficiency in the *Npc1*<sup>-/-</sup> mouse model resulted in a perturbation of transition metal homeostasis in the plasma and key organs (brain, liver, spleen, heart, lungs, and kidneys). Analysis of human patient CSF, plasma and post-mortem brain tissues also indicated disrupted metal homeostasis. There was a disparity in the direction of metal changes between the human and the *Npc1*<sup>-/-</sup> mouse samples, which may reflect species-specific metal metabolism. Nevertheless, common to both species is brain zinc accumulation. Furthermore, treatment with the glucosylceramide synthase inhibitor miglustat, the only drug shown in a controlled clinical trial to have some efficacy for NP-C1, did not correct the alterations in CSF and plasma transition metal and ceruloplasmin (CP) metabolism in NP-C1 patients. These findings highlight the importance of NPC1 function in metal homeostasis, and indicate that metal-targeting therapy may be of value as a treatment for NP-C.

## INTRODUCTION

Niemann-Pick Disease Type C (NP-C) is an autosomal recessive lysosomal lipid storage disorder with progressive neurodegeneration. NP-C is classified as type C1 (NP-C1; OMIM 257220) or type C2 (NP-C2; OMIM 607625), which are caused by mutations in the *NPC1* or *NPC2* gene, respectively<sup>1,2</sup>. Mutations in the *NPC1* gene accounts for 95% of NP-C patients<sup>3</sup>. The concerted activities of NPC1 and NPC2 proteins are essential to intracellular mobilization of unesterified cholesterol and other lipids<sup>4,5</sup>. Loss of either NPC1 or NPC2 function results in distinctive intracellular accumulation of cholesterol and glycosphingolipids in late endosomes and lysosomes. The onset of the disease can occur at any age, but it typically manifests in childhood with an early death by adolescence. Degeneration of cerebellar Purkinje neurons is a prominent early feature in the disease progression, which leads to clinical symptoms of motor impairments that include cerebellar ataxia, dysarthria and dysphagia<sup>3</sup>. Dementia is a late stage feature of NP-C due to the loss of hippocampal and cortical neurons<sup>6-8</sup>.

Transition metals such as iron, manganese, copper, and zinc are integral to diverse biological processes including neurotransmission, myelination, synaptogenesis, DNA transcription, respiration, and antioxidant defense. Dysregulation of essential redox-active metals such as copper and iron, can enhance toxic Fenton and Haber-Weiss reactions, and generate reactive oxygen species (ROS)<sup>9</sup>. Oxidative stress is a pathological feature of NP-C<sup>10-14</sup>. Notably, there is an elevation of non-enzymatically produced oxysterols in NP-C<sup>15</sup>, which could be a product of perturbed metal homeostasis.

Emerging data indicate an imbalance of metal ions in NP-C1. Skin fibroblast cells derived from NP-C1 patients have up-regulated gene expression of metalloproteins involved in copper (copper-transporting ATPase 1 (ATP7A)), iron (ferritin and sideroflexin 1) and zinc (zinc

transporter ZIP2) metabolism<sup>11</sup>. Recent studies reported elevated copper levels in the liver and plasma of the *Npc1*<sup>-/-</sup> mouse model, concomitant with an increase in plasma ceruloplasmin (CP) levels<sup>12, 16</sup>. However, these findings are inconsistent with a case report of an NP-C1 patient who had elevated serum free copper with low CP<sup>17</sup>. An alternative explanation is that the low serum CP in this patient results from defective NPC1-dependent trafficking of the copper transporter ATP7B in hepatic cells from the late endosomes to the secretory pathway<sup>18, 19</sup>, where ATP7B facilitates copper incorporation into CP. CP plays an important role in iron export<sup>20</sup>. There is a lack of ferritin immunoreactivity in spleen, liver, and fetal tissues from human NP-C cases, suggesting that tissue iron is not properly regulated in NP-C<sup>21-23</sup>. Collectively, these findings implicate disrupted metal homeostasis in the *Npc1*<sup>-/-</sup> mouse model and NP-C1 patients, yet there is a lack of a detailed metal analysis of NP-C1 tissues and biological fluids to resolve the conflicting findings. To address this deficiency, we present here a detailed transition metal analysis of cerebrospinal fluid (CSF), plasma and tissue samples from human NP-C1 patients and the *Npc1*<sup>-/-</sup> mouse model.

## EXPERIMENTAL

### Animals

The *Npc1*<sup>-/-</sup> mouse model (BALB/c *Npc1*<sup>nih</sup>)<sup>24</sup> was obtained from Jackson Laboratories and maintained on a standard chow diet. Experimental procedures were approved by the Washington University Animal Studies Committee and were conducted in accordance with the USDA Animal Welfare Act and the Public Health Service Policy for the Humane Care and Use of Laboratory Animals. Postnatal day 21 (P21) and day 49 (P49) female mice were anesthetized using a cocktail of telazol/butophanol/dexmedetomidine, followed by exsanguination and transcardial perfusion. Plasma samples were prepared from *Npc1*<sup>-/-</sup> and

wild-type littermate control mice sacrificed at P21 (n = 5/genotype) and P49 (n = 18/genotype), using sodium heparin as the anti-coagulant. The following organs were collected (n = 14/genotype): cerebellum, cerebrum, liver, spleen, lungs, kidneys, and heart. Plasma and tissue samples were snap frozen in liquid nitrogen and stored at -80°C until use. The investigators were blinded to the sample genotype. Samples were decoded at the completion of metal analysis.

### **Human tissue and biological fluid samples**

Post-mortem human brain tissues (cerebellum and hippocampus) from NP-C cases and matched non-NP-C control subjects (n (hippocampus) = 5/diagnostic group; n (cerebellum) = 4/diagnostic group); Table S3) were obtained from the Eunice Kennedy Shriver National Institute of Child Health and Development (NICHD) Brain and Tissue Bank for Developmental Disorders (MD, USA). NP-C1 patient cerebrospinal fluid (CSF) samples were collected under approved protocols from NICHD (IRB# 06-CH-0186; n = 21; Table S5) and Children's Hospital & Research Center Oakland (IRB# 2010-70) Institutional Review Boards (n = 2, not included in data analysis). Informed consent and assent, when appropriate, were obtained. The lumbar puncture was performed under sedation. CSF was collected in polypropylene tubes, snap frozen on dry ice, and stored at -80°C until use. NP-C1 patient and healthy control (HC) plasma samples were collected under approved protocols from NICHD Institutional Review Board (IRB# 06-CH-0186; n (HC) = 34; n (NP-C1) = 33) and Melbourne Health Human Research Ethics Committee (QA2010057; n = 7/diagnostic group). Metal and biochemical analyses of human brain tissue and biological fluid samples were approved by the University of Melbourne Human Research Ethics Committee (HREC# 1034015).

## Metal analysis

Metal content in CSF, plasma and tissues samples were analyzed using inductively-coupled plasma mass spectrometry (ICP-MS) as previously described<sup>25</sup>. Lyophilized human and murine tissue (~40 – 600 mg wet weight or ~5 – 40 mg dry weight), CSF (100  $\mu$ L) and plasma (50  $\mu$ L) samples were pre-digested overnight in 50  $\mu$ L of concentrated HNO<sub>3</sub> (Aristar Grade, BDH), followed by heating to 90°C for 20 min. The acid digested tissue, CSF and plasma samples were diluted with 1% HNO<sub>3</sub>, and metal content was measured using a 7700x ICP-MS (Agilent). The instrument was calibrated using certified ICP-MS standard solutions (AccuStandard) containing 0, 10, 50, 100, and 500 ppb of all elements measured in 1% HNO<sub>3</sub>. Metal content in limited CSF samples were confirmed by inductively-coupled plasma optical emission spectrometry (ICP-OES)<sup>26</sup> (data not shown). For ICP-OES analysis, the CSF sample (1 mL) was digested overnight in OmniTrace 70% HNO<sub>3</sub> (EMD) with heating at 60°C and shaking at 200 rpm, then diluted to 5% HNO<sub>3</sub> with OmniTrace water. Then the samples were analyzed for elemental analysis (similar to ICP-MS) using a Vista Pro ICP-OES (Varian, Inc). Elemental values were calibrated using National Institute of Standards and Technology (NIST)-traceable elemental standards and validated using NIST-traceable 1577b bovine liver reference material. Cesium (50 ppm) was used for ionization suppression and yttrium (5 ppm) was used as an internal standard. Data was collected and summarized using native software (ICP Expert; Varian, Inc).

## Quantification of ceruloplasmin

Western blotting was used to identify total, apo- and holo-CP in both CSF and plasma samples as previously described<sup>27</sup>. Heparinized plasma samples were diluted 100-fold with

0.9% saline (Baxter). For each diluted heparinized plasma or neat CSF sample, two 5  $\mu$ L preparations per sample were made. One set was heated at 95°C for 5 min for the detection of total CP, and the other set was not heat treated for differential detection of apo- and holo-CP. Protein samples were separated by SDS-PAGE using either 4 – 12% BisTris gradient gels (Invitrogen) or 4 – 20% Criterion TGX™ gels (Bio-Rad), using either MOPS (Invitrogen) or Tris/Glycine/SDS (Bio-Rad) running buffer, respectively. After separation by SDS-PAGE, proteins were transferred to a 0.2  $\mu$ m nitrocellulose or PVDF membrane (Bio-Rad) using either an iBlot® Dry Blot System (Invitrogen) or Trans-Blot® Turbo™ Transfer System (Bio-Rad). Blots were blocked with Tris-buffered saline containing 0.05% Tween® 20 (Sigma) and 5% skim milk, and probed with anti-human ceruloplasmin antibody (Dako) diluted in the blocking buffer. The blots were subsequently incubated with an anti-rabbit IgG-horseradish peroxidase conjugated secondary antibody (Dako). Blots were developed using an ECL™ Western blotting detection system (Millipore), and visualized using an LAS-3000 Imaging System (Fujifilm). Densitometry quantification of immunoreactive signals was performed using MultiGauge v.3 (Fujifilm). CP concentration was estimated against purified human CP (Vital Products) standards.

### **Plasma ceruloplasmin oxidase activity**

Plasma ceruloplasmin oxidase activity was assayed using a modified protocol for 96-well plates based on that previously described<sup>28</sup>. Briefly, 5  $\mu$ L of each plasma sample was pre-incubated at 37°C with 75 mM sodium acetate buffer (pH 5.0) with or without 1 mM sodium azide. The reaction was initiated with the addition of 20  $\mu$ L of 1.58 mM *o*-dianisidine dihydrochloride (Sigma). Samples on duplicate plates were incubated at 37°C for 5 min or 60

min. At designated time points, the reaction was stopped with 200  $\mu$ L of 9 M sulfuric acid. The absorbance at 540 nm of the oxidized product was measured using a PowerWave microplate spectrometer (BioTek). CP oxidase activity was calculated as the difference between the total and azide-resistant oxidase activities.

### Statistical analysis

Human clinical data analyses were performed with R version 2.15.2<sup>29</sup>, using the following packages, multcomp<sup>30</sup>, effects<sup>30</sup> and ggplot2<sup>31</sup>. The data were checked for normality. Those that showed a deviation were transformed as required by BoxCox transformation<sup>32</sup>. For categorical variables such as gender, a chi-square test was performed to assess the distribution across the defined groups. Analysis of variance was used to assess any age difference between the groups. For all other continuous variables, analysis of co-variance (ANCOVA) was performed, adjusting for age (as a continuous variable), gender, clinical group and cohort site. Pairwise comparisons were performed using the Tukey contrasts with false discovery correction. Fisher's exact test was used to assess the significance of the difference in frequency of subjects below the reference range between the clinical groups. Multiple linear regression analysis was performed to assess the relationship between continuous variables (*e.g.* copper and CP levels) under investigation. The analysis included examination of the interaction between gender and miglustat status, gender and continuous variables, and miglustat status and continuous variables. We included only the significant interactions ( $p < 0.05$ ) in the final model.

Statistical analyses of animal data, Student's *t*-test or two-way analysis of variance (ANOVA) with Bonferroni correction for multiple comparisons, as indicated in figure legends,

were performed using GraphPad Prism version 5.04 for Windows (GraphPad Software). Data are presented as mean  $\pm$  S.D. or mean  $\pm$  S.E.M. as indicated. Statistical significance was defined as \*  $p \leq 0.05$ ; \*\*  $p \leq 0.01$ ; \*\*\*  $p \leq 0.001$ .

## RESULTS

### Extensive metal dyshomeostasis in tissues of *Npc1*<sup>-/-</sup> mice

To assess the impact of *NPCL1* gene ablation on metal metabolism, we analyzed metal contents in the *Npc1*<sup>-/-</sup> (BALB/c *Npc1*<sup>nih</sup>)<sup>24</sup> mice, a well-characterized model for NP-C1. Brain, liver, spleen, lungs, heart, and kidneys, were collected from symptomatic female *Npc1*<sup>-/-</sup> and wild-type (WT) littermate control mice at P49. Metal analysis by inductively-coupled plasma mass spectrometry (ICP-MS) revealed marked changes in *Npc1*<sup>-/-</sup> tissues compared to WT controls (Figure 1 and Table S1).

Iron levels were significantly decreased in *Npc1*<sup>-/-</sup> liver ( $29 \pm 5\%$ ;  $p < 0.0001$ ) and spleen ( $18 \pm 4\%$ ;  $p < 0.0001$ ) compared to WT. These results were consistent with previous studies that reported a lack of ferritin in these tissues from human NP-C cases<sup>21-23</sup>, indicating a functional iron deficiency. In contrast, we found a moderate iron accumulation in the cerebellum ( $16 \pm 3\%$ ;  $p < 0.0001$ ) and cerebrum ( $22 \pm 2\%$ ;  $p < 0.0001$ ) of *Npc1*<sup>-/-</sup> mice. There was no difference in iron levels in the lung, heart and kidney.

Copper levels were significantly altered in each tissue analyzed. Copper was significantly increased in the liver ( $23 \pm 4\%$ ;  $p < 0.0001$ ) and in the lung ( $170 \pm 17\%$ ;  $p < 0.0001$ ) of *Npc1*<sup>-/-</sup> mice compared to WT. A moderate but significant copper deficiency was observed in all other tissues examined, with reductions in *Npc1*<sup>-/-</sup> cerebellum ( $16 \pm 3\%$ ;  $p < 0.0001$ ), cerebrum ( $15 \pm 2\%$ ;  $p < 0.0001$ ), spleen ( $10 \pm 4\%$ ;  $p = 0.01$ ), kidney ( $14 \pm 2\%$ ;  $p < 0.0001$ ), and

heart ( $6 \pm 2\%$ ;  $p = 0.009$ ). The elevation of copper in the *Npc1*<sup>-/-</sup> mouse liver was consistent with previous reports<sup>12, 16</sup>. It should be noted that despite a close agreement in the mean cerebellar copper concentrations measured in our study and that by Vazquez *et al*<sup>16</sup>, there was a discrepancy in our statistical significance testing results. Our study, but not Vazquez *et al*, found a significant decrease ( $16 \pm 3\%$ ) in cerebellar copper concentrations in *Npc1*<sup>-/-</sup> compared to WT. This variance may be explained by our smaller error values and that the study by Vazquez *et al* may be under-powered due to a smaller *Npc1*<sup>-/-</sup> sample size. Methodological differences may have also contributed to the discrepant result.

Zinc levels were increased in the *Npc1*<sup>-/-</sup> mouse cerebellum ( $14 \pm 3\%$ ;  $p < 0.0001$ ) and cerebrum ( $12 \pm 2\%$ ;  $p < 0.0001$ ) relative to WT. The liver ( $24 \pm 2\%$ ;  $p < 0.0001$ ) and the lung ( $28 \pm 6\%$ ;  $p < 0.0001$ ) of *Npc1*<sup>-/-</sup> mice were markedly decreased in zinc, and to a lesser extent in the spleen ( $7 \pm 3\%$ ;  $p = 0.03$ ) and kidney ( $9 \pm 2\%$ ;  $p < 0.0001$ ), compared to WT.

There was a significant accumulation of manganese content in the cerebellum ( $23 \pm 3\%$ ;  $p < 0.0001$ ) and cerebrum ( $21 \pm 3\%$ ;  $p < 0.0001$ ) of *Npc1*<sup>-/-</sup> mice compared to WT. Manganese was also significantly increased to a lesser extent in the spleen ( $14 \pm 7\%$ ;  $p = 0.03$ ) and the heart ( $7 \pm 3\%$ ;  $p = 0.02$ ) of *Npc1*<sup>-/-</sup> mice. In contrast, there was a reduction in the *Npc1*<sup>-/-</sup> mouse liver ( $14 \pm 2\%$ ;  $p < 0.0001$ ) and lung ( $15 \pm 6\%$ ;  $p = 0.02$ ) manganese concentration.

#### Aberrant metal levels and ceruloplasmin abnormalities in *Npc1*<sup>-/-</sup> mice plasma

We analyzed the metal content of plasma samples collected from pre- and symptomatic female *Npc1*<sup>-/-</sup> and WT littermate control mice at P21 and P49, respectively. There was a trend to an age-dependent rise in plasma iron concentration in both genotypes, but not statistically significant (Figure 2A and Table S2). Our observation of a  $34 \pm 7\%$  increase ( $p < 0.0001$ ) in

plasma copper at P49 in *Npc1*<sup>-/-</sup> mice compared to WT (Figure 2B and Table S2) was consistent with that previously reported<sup>16</sup>. Furthermore, we identified a marked age-dependent elevation of plasma copper in *Npc1*<sup>-/-</sup> mice that was not observed in WT animals (Figure 2B and Table S2). In contrast, we found an elevation in plasma zinc in pre-symptomatic *Npc1*<sup>-/-</sup> mice at P21 (Figure 2C and Table S2). At the symptomatic age of P49, plasma zinc in *Npc1*<sup>-/-</sup> mice fell to a level comparable to that of WT.

CP is a key protein linked to both copper and iron metabolism<sup>33</sup>. It requires six copper atoms to form the stable and active holo-CP species<sup>34</sup>, which is central to its ferroxidase activity and cellular iron export by catalyzing the oxidation of ferrous to ferric iron<sup>35</sup>. Therefore, impaired copper homeostasis can negatively affect the synthesis and activity of holo-CP, and subsequently iron homeostasis. We quantified total, apo- and holo-CP levels in the plasma by western blotting (Figure S1). In parallel with the elevated plasma copper levels at P49 in *Npc1*<sup>-/-</sup> mice, we also observed a  $49 \pm 4\%$  increase ( $p = 0.0004$ ) in total CP compared to WT (Figure 2D). This was also reflected in a concomitant  $53 \pm 7\%$  increase ( $p < 0.0001$ ) in total oxidase activity, the sum of azide-sensitive activity (attributed to CP, and known as ferroxidase I) and azide-resistant activity (ferroxidase II, which is proportionally more in mice than in humans)<sup>36</sup> (Figure 2E). Although there was no age-dependent change in total CP levels in *Npc1*<sup>-/-</sup> mice, there was an age-dependent increase in the copper-bound active holo-CP level and a decrease in the unmetallated apo-CP level (Figure 2F). These changes in apo- and holo-CP levels were reflected in the age-dependent increase in total (azide-sensitive plus -insensitive) and CP oxidase (azide-sensitive) activities observed in *Npc1*<sup>-/-</sup> mouse plasma (2E and 2G).

### Zinc accumulates in the human NP-C disease patient cerebellum

To assess the potential of dysregulated metal homeostasis to be a contributing factor to neurodegeneration in NP-C patients, we analyzed the metal content of brain tissues, CSF and plasma. The cerebellum and hippocampus have significant neuropathology in NP-C disease<sup>6-8</sup>. We obtained post-mortem cerebellar (n = 4/diagnostic group) and hippocampal (n = 5/diagnostic group) tissues from NP-C cases and matched non-NP-C controls (Table S3). Limited availability of post-mortem NP-C disease brain tissue samples restricted the power of this study. While the sample sizes are small, and having determined that there were no effects of gender or age, these factors were not included in the analysis of data presented. We found a significant elevation of zinc ( $28 \pm 10\%$ ;  $p = 0.03$ ) in NP-C cerebellar tissue compared to non-NP-C control tissues (Figure 3 and Table S4). There was a possible trend to elevated iron levels in the NP-C cerebellum compared to controls ( $p = 0.06$ ). In the hippocampus, there was no significant difference in transition metals measured between NP-C and control samples, but a possible trend towards an increase in zinc ( $p = 0.09$ ).

### NP-C1 cerebrospinal fluid is deficient in transition metal

We also evaluated CSF transition metal levels in 21 NP-C1 disease patients. A third of the NP-C1 subjects were treated with miglustat (Table S5), an inhibitor of glycosphingolipid synthesis and the only drug shown in a controlled clinical trial to have some efficacy for NP-C<sup>37, 38</sup>. Therefore, we also analyzed the effect of miglustat treatment on CSF metal levels. Since control CSF samples from healthy individuals, particularly pediatric samples, are impractically rare, we used published reference range values<sup>39</sup> as a comparison for the NP-C1 CSF metal levels.

Relative to the reference range, the majority of the NP-C1 CSF samples analyzed were deficient in the essential transition metals iron, copper and zinc (Figure 4B, 4C, 4D and Table S5). The mean CSF manganese concentration was just below the lower reference limit (Figure 4A; Table S5). Miglustat treatment had no effect on CSF metal concentrations. There was no association between levels of these metal ions and disease severity or age. The deficiency of transition metals was confirmed using samples that were measured in a separate lab using inductively-coupled plasma optical emission spectrometry (ICP-OES; data not shown). The apparent deficiency of transition metals in the CSF may indicate a failure of essential metal homeostasis in the central nervous system of NP-C1 patients.

#### CSF ceruloplasmin levels correlate with NP-C1 disease severity

To determine whether the apparent CSF copper and iron deficiencies affect the level of CP in the CSF of NP-C1 patients, we quantified CSF total, apo- and holo-CP levels by western blotting (Figure S2A). It was noteworthy that, despite an apparent copper deficiency in the CSF, the estimated CSF total CP concentration in NP-C1 patients was slightly higher than the reference range (Table S5). We found a significant positive correlation between NP-C1 disease severity and CSF total CP and holo-CP concentrations (Figure 5A). An increase in 1 nM of total CP and holo-CP corresponded to an increase of  $2 \pm 1$  and  $2.7 \pm 0.9$  points in clinical severity score<sup>40</sup>, respectively. Thus, CSF total CP and holo-CP may be useful biomarkers of NP-C1 disease progression.

We further examined the association between CSF CP species with CSF metal ions. Unlike plasma, there was no correlation between copper and total CP or holo-CP in the NP-C1 CSF samples (Figure 5B). Interestingly, we found a modest, but significant negative correlation

between copper and apo-CP (Figure 5B). We also found significant negative correlations between NP-C1 CSF manganese and total CP or holo-CP levels, which was independent of miglustat treatment (Figure 5C). These relationships were adjusted for age and gender.

#### Significantly decreased plasma metal concentrations in NP-C1

Next, we appraised NP-C1 patient plasma metal levels. We found, compared to matched non-NP-C healthy controls (HC), NP-C1 cases had slightly lower plasma manganese, iron and zinc (Figure 6 and Table S6). In particular, values below the reference range for plasma zinc were frequent in NP-C1 patients (12%), and uncommon in the HC (5%;  $p = 0.04$ ). Miglustat treatment did not impact on any of these changes. Although there was a slight decrease in the plasma copper concentration in the NP-C1 cases, the mean concentration difference was not statistically different to that of HC (Table S6).

#### Miglustat treatment affects holo-CP formation and specific oxidase activity

CP is a major copper-carrying protein in the blood<sup>41, 42</sup>, and it is sometimes used as an indirect indicator of serum and plasma copper levels. On the basis of the disparate findings of serum/plasma copper changes between our study and a case study that reported an elevation in serum free copper<sup>17</sup>, we further investigated the change in human plasma CP. We found that there was no significant difference in plasma total CP concentration between HC and both NP-C1 groups (Figure 7A, Figure S2B and Table S6). However, further separating CP into the active copper-bound holo-CP and unmetallated apo-CP species, we found that miglustat treatment resulted in a small, but significant, increase in plasma holo-CP concentration in the

NP-C1 patients (Figure 7B and Table S6), while there was no difference in the mean apo-CP concentration between the three groups (Figure 7C and Table S6).

Stable and active CP requires binding of six copper atoms<sup>34</sup>. Our calculation of the mean plasma Cu:total CP and Cu:holo-CP ratios for HC approximated the expected ratio of six (Figure 7D, 7E and Table S6). Consistent with the plasma copper data, the plasma Cu:total CP and Cu:holo-CP ratios for NP-C1 patients not treated with miglustat did not deviate significantly from that of the HC (Figure 7D and 7E). It is noteworthy that NP-C1 patients treated with miglustat had significantly decreased plasma Cu:total CP and Cu:holo-CP ratios compared to HC and NP-C1 patients not treated with miglustat (Figure 7D and 7E). The decrease in plasma Cu:holo-CP ratio in NP-C1 patients treated with miglustat was paralleled by a small but significant decrease in holo-CP specific oxidase activity (Figure 7F).

Interestingly, we found a negative association between NP-C1 disease severity and plasma apo-CP concentration that was gender-dependent (female only) but miglustat-independent (Figure 7G). However, there was a significant difference in severity score that was miglustat-dependent after adjusting for gender and apo-CP concentration ( $p < 0.0002$ ). Overall, NP-C1 patients treated with miglustat had lower severity score compared to those not treated with miglustat. There was no association between NP-C1 disease severity and other CP or CP activity parameters examined.

## DISCUSSION

To our knowledge, this is the first comprehensive transition metal analysis of tissue and plasma samples from NP-C1 patients and an *Npc1*<sup>-/-</sup> mouse model. Our study shows an extensive perturbation of metal homeostasis in the plasma and major organs and plasma CP homeostasis in the *Npc1*<sup>-/-</sup> mouse model compared to WT. We also found disturbed metal

homeostasis in human NP-C1 patient CSF, post-mortem cerebellar tissue, and plasma samples. Collectively, disrupted metal homeostasis in the human NP-C1 clinical samples and the *Npc1*<sup>-/-</sup> mouse model indicates a critical role for NPC1 in the regulation of metal metabolism. It is important to note that the *Npc1*<sup>-/-</sup> mouse model does not fully recapitulate the changes in metal and CP homeostasis found in NP-C1 patients, but common to both species is the aberrant zinc homeostasis in the brain.

A number of factors can contribute to the disparity between the *Npc1*<sup>-/-</sup> mouse model and human NP-C1 clinical sample data. The *Npc1*<sup>-/-</sup> mouse model is effectively a “knockout” of *Npc1* due to a large 703 bp deletion in the gene<sup>24</sup>, representing the most severe phenotype. In comparison, most of the human NP-C1 patients harbor missense mutations in the *NPC1* gene with pleiotropic phenotypes<sup>43,44</sup>, which may exhibit mild to moderate phenotypes relative to the residual protein activity. However, due to the small human sample size, the statistical power was low and precludes the inclusion of specific mutations as a part of the statistical model analysis. Furthermore, changes in metal metabolism in human NP-C1 patients may be obscured by heterogeneous genetic backgrounds and environmental factors. For example, the biochemical manifestations and the age of disease onset in the NP-C1 patients may be modified by additional genetic factors, such as the *Apo-ε4* genotype<sup>45</sup>. It is noteworthy that ApoE binds transition metals, with highest affinity for copper<sup>46</sup>. The combination of cysteine and arginine at the isoform-defining positions 112 and 158 may result in differential metal metabolism in NP-C1 patients. Moreover, metal metabolism in humans is sensitive to variations in diet and intake of supplements/drugs that would not be a consideration in laboratory mice.

Peripheral copper dyshomeostasis has been associated with a loss of NPC1 function in an NP-C1 patient and the *Npc1*<sup>-/-</sup> mouse model<sup>11, 12, 16, 17</sup>. We observed no significant difference in

plasma copper level in the present NP-C1 patient cohort compared to HC (Table S6). However, we did observe a late-disease stage increase in plasma copper in *Npc1*<sup>-/-</sup> mice (Figure 2B) as previously reported<sup>16</sup>. This rise in plasma copper coincides with a significant increase in late-disease stage hepatic oxidative gene expression<sup>13</sup>. Thus, copper is likely a contributor to the rise in oxidative stress in *Npc1*<sup>-/-</sup> mice. Disrupted copper homeostasis is widespread in all *Npc1*<sup>-/-</sup> mouse tissue types examined, with the most dramatic change of a  $170 \pm 17\%$  increase in the lungs. It is possible that the copper-induced oxidative stress in the lungs may contribute to the pulmonary abnormalities reported in animal model studies<sup>47,48</sup>.

CP is a multi-copper oxidase that plays an important role in copper and iron metabolism, and it may serve as a surrogate peripheral marker of copper status. Consistent with our finding of normal plasma copper levels in NP-C1 patients, the plasma levels of all CP species, holo-CP oxidase activity and Cu:holo-CP ratio analyzed in this study remained unchanged between the HC and the NP-C1 patients not taking miglustat (Figure 7 and Table S6). However, there was a small but significant decrease in plasma iron compared to HC (Figure 6B and Table S6) that cannot be explained by the apparent normal holo-CP activity. It should be noted that despite an apparent increase in holo-CP in NP-C1 patients treated with miglustat, the Cu:holo-CP ratio and holo-CP specific activity were significantly decreased compared to NP-C1 patients not treated with miglustat and compared to HC. The negative impact of miglustat on CP specific activity suggests that glycosphingolipids may be important in regulating CP activity by an uncertain mechanism. Again, in contrast to the human data, and as previously reported<sup>16</sup>, there is a concomitant elevation of the plasma total CP level in symptomatic *Npc1*<sup>-/-</sup> mice (Figure 2D). In this study we further demonstrated that this corresponds to increased copper-bound holo-CP and CP oxidase activity (Figure 2F and 2G). This difference between human and mouse plasma CP

and its oxidase activity may be explained by a species-specific difference in CP metabolism and activity<sup>36</sup>. In humans, CP accounts for 90 – 100% of the plasma ferroxidase activity. In contrast, only about 50% of mouse plasma ferroxidase is attributable to CP, while the source of the remaining 50% is unknown. Furthermore, our *in vivo* human and mouse CP data do not support the *in vitro* finding that NPC1 regulates ATP7B trafficking to the secretory pathway, where ATP7B incorporates copper into CP<sup>18, 19</sup>. Further studies are required to resolve this apparent inconsistency.

Interestingly, there is an apparent copper deficiency in the CSF of NP-C1 patients, but a slightly higher total CP level compared to their respective reference ranges. There is a lack of association between CSF total and holo-CP with copper (Figure 5B), and the CSF Cu:CP ratio is 7 – 8-folds greater than that observed in the plasma. Our finding is consistent with an earlier study that reported only a small fraction of copper is associated with CP in the CSF in both Alzheimer's disease (AD) and control subjects<sup>49</sup>. We have limited knowledge of normal CP metabolism in the CSF, but the difference between peripheral and CSF Cu:CP ratios suggests discrete CP metabolism in these compartments. Collectively, these findings are consistent with the hypothesis that, unlike the plasma, the majority of the CSF copper is not CP-bound but binds to an yet-to-be-identified ligand<sup>50</sup>. However, in contrast to decreased CSF holo-CP in AD, our analysis of the NP-C1 CSF revealed a modest but significant positive association between CSF total and holo-CP concentrations and disease severity (Figure 5A). CP is an acute phase marker and this association may reflect the increase in neuroinflammation in NP-C1<sup>51</sup>. Thus CSF CP may be a useful biomarker to monitor the disease progression and therapeutic response, in addition to the other CSF neuroinflammatory markers identified in the Cologna *et al* study<sup>51</sup>.

Zinc is an essential trace element important to the development and survival of all organisms. It is particularly critical to the normal brain function, such as neurotransmission and signaling<sup>52, 53</sup>. In *Npc1*<sup>-/-</sup> mice, there was an early, pre-symptomatic increase in plasma zinc compared to WT animals at P21, which appeared to normalize by P49 (Figure 2C and Table S1). Interestingly, an MRI study has revealed that pre-symptomatic 3-week old *Npc1*<sup>-/-</sup> mice exhibit a loss of white matter<sup>54</sup>. Combined with the age-dependent increase in plasma copper in symptomatic *Npc1*<sup>-/-</sup> mice at P49, the observed changes in plasma copper and zinc could serve as pre- and symptomatic biomarkers in the *Npc1*<sup>-/-</sup> mouse model. However, in NP-C1 patients, plasma zinc is significantly decreased compared to HC and they are more frequently below the reference range (Figure 6C and Table S6). Also, this apparent zinc deficiency is not corrected by miglustat treatment. It is noteworthy that hepatosplenomegaly is associated with human serum/plasma zinc deficiency<sup>55, 56</sup>, and is a complication of NP-C. Despite the inconsistencies in changes in plasma zinc between NP-C1 patients and *Npc1*<sup>-/-</sup> mice, both species demonstrate brain zinc overload (Figure 1 and 3, Tables S1 and S4). Excess brain zinc can promote tau expression, phosphorylation and aggregation, possibly contributing to the formation of pathological neurofibrillary tangles (NFTs) in NP-C<sup>57-63</sup>. Furthermore, zinc also accumulates in brain tissues from ovine and murine models of CLN6 neuronal ceroid lipofuscinosis (Batten disease), a lysosomal storage disease<sup>64, 65</sup>. Thus, brain zinc accumulation<sup>64, 65</sup> is an emerging common pathological feature associated with neurodegeneration in lysosomal storage disorders.

## CONCLUSIONS

The findings in this study support a novel role for NPC1 in the regulation of metal metabolism, although its impact on human and mouse metal metabolism may differ. We hypothesize that since the lysosome is believed to play a critical role in the uptake and sorting of

transition metals<sup>66</sup>, the lesion of *NPCI* may perturb metal homeostasis by disrupting lysosomal-dependent sorting mechanisms. It is notable that miglustat does not correct the perturbed plasma manganese, iron and zinc levels and disrupts plasma CP chemistry in NP-C1 patients. Future therapeutic strategies for NP-C1 may need to consider the failure in metal metabolism to improve treatment efficacy.

## ACKNOWLEDGEMENTS

This work was supported by grants from the National Health & Medical Research Council of Australia (A.I.B.), Cooperative Research Centre for Mental Health (A.I.B.), the Addi and Cassi Fund (A.I.B. and Y.H.H.), Perpetual Trustees (Harry Secomb Foundation and Payne L & Heather Medical Research Charitable Foundation (A.I.B.)), intramural research program of the Eunice Kennedy Shriver National Institute of Child Health and Human Development (F.D.P.), Ara Parseghian Medical Research Foundation (D.S.O. and F.D.P.), Dana's Angels Research Trust (D.S.O. and F.D.P.). Bench to Bedside award from the NIH Clinical Center and Office of Rare Diseases (F.D.P.). The Florey Institute of Neuroscience and Mental Health acknowledges the strong support from the Victorian Government and in particular the funding from the Operational Infrastructure Support Grant.

The authors thank Shih-Min Chiu, Amelia Sedjahtera, Lisa Bray, Kali Hubbert, Charlotte Jordan, Tai Holland, and the Australian Imaging, Biomarker and Lifestyle (AIBL) Study research team (Brett Trounson, Christopher Fowler, Rebecca Rumble and Kelly Pertile) for technical support; and Dr. Paul Adlard (Florey Institute of Neuroscience and Mental Health) for provision of non-NP-C control CSF samples. The authors would like to thank NP-C patients and their families, and healthy control subjects for their contribution and participation in this study.

## CONFLICT OF INTEREST STATEMENT

A.I.B. is a shareholder in Prana Biotechnology Ltd, Cogstate Ltd, and Mesoblast Ltd.

## REFERENCES

1. E. D. Carstea, J. A. Morris, K. G. Coleman, S. K. Loftus, D. Zhang, C. Cummings, J. Gu, M. A. Rosenfeld, W. J. Pavan, D. B. Krizman, J. Nagle, M. H. Polymeropoulos, S. L. Sturley, Y. A. Ioannou, M. E. Higgins, M. Comly, A. Cooney, A. Brown, C. R. Kaneski, E. J. Blanchette-Mackie, N. K. Dwyer, E. B. Neufeld, T. Y. Chang, L. Liscum, J. F. Strauss, 3rd, K. Ohno, M. Zeigler, R. Carmi, J. Sokol, D. Markie, R. R. O'Neill, O. P. van Diggelen, M. Elleder, M. C. Patterson, R. O. Brady, M. T. Vanier, P. G. Pentchev and D. A. Tagle, *Science*, 1997, **277**, 228-231.
2. S. Naureckiene, D. E. Sleat, H. Lackland, A. Fensom, M. T. Vanier, R. Wattiaux, M. Jadot and P. Lobel, *Science*, 2000, **290**, 2298-2301.
3. M. C. Patterson, E. Mengel, F. A. Wijburg, A. Muller, B. Schwierin, H. Drevon, M. T. Vanier and M. Pineda, *Orphanet J Rare Dis*, 2013, **8**, 12.
4. M. T. Vanier, *Orphanet J Rare Dis*, 2010, **5**, 16.
5. A. I. Rosenbaum and F. R. Maxfield, *J Neurochem*, 2011, **116**, 789-795.
6. S. Love, L. R. Bridges and C. P. Case, *Brain*, 1995, **118 ( Pt 1)**, 119-129.
7. W. Y. Ong, U. Kumar, R. C. Switzer, A. Sidhu, G. Suresh, C. Y. Hu and S. C. Patel, *Exp Brain Res*, 2001, **141**, 218-231.
8. A. Yamada, M. Saji, Y. Ukita, Y. Shinoda, M. Taniguchi, K. Higaki, H. Ninomiya and K. Ohno, *Brain Dev*, 2001, **23**, 288-297.
9. B. Halliwell and J. M. C. Gutteridge, *Biochem. J.*, 1984, **219**, 1-14.
10. R. Fu, N. M. Yanjanin, S. Bianconi, W. J. Pavan and F. D. Porter, *Mol Genet Metab*, 2010, **101**, 214-218.
11. J. V. Reddy, I. G. Ganley and S. R. Pfeffer, *PLoS ONE*, 2006, **1**, e19.

12. M. C. Vazquez, T. del Pozo, F. A. Robledo, G. Carrasco, L. Pavez, F. Olivares, M. Gonzalez and S. Zanlungo, *PLoS ONE*, 2011, **6**, e28777.
13. C. V. Cluzeau, D. E. Watkins-Chow, R. Fu, B. Borate, N. Yanjanin, M. K. Dail, C. D. Davidson, S. U. Walkley, D. S. Ory, C. A. Wassif, W. J. Pavan and F. D. Porter, *Hum Mol Genet*, 2012, **21**, 3632-3646.
14. R. Fu, C. A. Wassif, N. M. Yanjanin, D. E. Watkins-Chow, L. L. Baxter, A. Incao, L. Liscum, R. Sidhu, S. Firnkens, M. Graham, D. S. Ory, F. D. Porter and W. J. Pavan, *Hum Mol Genet*, 2013.
15. F. D. Porter, D. E. Scherrer, M. H. Lanier, S. J. Langmade, V. Molugu, S. E. Gale, D. Olzeski, R. Sidhu, D. J. Dietzen, R. Fu, C. A. Wassif, N. M. Yanjanin, S. P. Marso, J. House, C. Vite, J. E. Schaffer and D. S. Ory, *Sci Transl Med*, 2010, **2**, 56ra81.
16. M. C. Vazquez, P. Martinez, A. R. Alvarez, M. Gonzalez and S. Zanlungo, *Biometals*, 2012, **25**, 777-786.
17. B. J. Connemann, M. Gahr, M. Schmid, H. Runz and R. W. Freudenmann, *J Clin Neurosci*, 2012.
18. C. Yanagimoto, M. Harada, H. Kumemura, H. Koga, T. Kawaguchi, K. Terada, S. Hanada, E. Taniguchi, Y. Koizumi, S. Koyota, H. Ninomiya, T. Ueno, T. Sugiyama and M. Sata, *Exp Cell Res*, 2009, **315**, 119-126.
19. C. Yanagimoto, M. Harada, H. Kumemura, M. Abe, H. Koga, M. Sakata, T. Kawaguchi, K. Terada, S. Hanada, E. Taniguchi, H. Ninomiya, T. Ueno, T. Sugiyama and M. Sata, *Hepatol Res*, 2011, **41**, 484-491.
20. A. C. Chua, R. M. Graham, D. Trinder and J. K. Olynyk, *Crit Rev Clin Lab Sci*, 2007, **44**, 413-459.

21. H. Christomanou and K. Harzer, *Biochem Mol Med*, 1996, **58**, 176-183.
22. H. Christomanou, J. Kellermann, R. P. Linke and K. Harzer, *Biochem Mol Med*, 1995, **55**, 105-115.
23. H. Christomanou, M. T. Vanier, P. Santambrogio, P. Arosio, W. J. Kleijer and K. Harzer, *Mol Genet Metab*, 2000, **70**, 196-202.
24. S. K. Loftus, J. A. Morris, E. D. Carstea, J. Z. Gu, C. Cummings, A. Brown, J. Ellison, K. Ohno, M. A. Rosenfeld, D. A. Tagle, P. G. Pentchev and W. J. Pavan, *Science*, 1997, **277**, 232-235.
25. C. J. Maynard, R. Cappai, I. Volitakis, R. A. Cherny, C. L. Masters, Q. X. Li and A. I. Bush, *J Inorg Biochem*, 2006, **100**, 952-962.
26. K. E. Page, K. N. White, C. R. McCrohan, D. W. Killilea and G. J. Lithgow, *Metalloomics*, 2012, **4**, 512-522.
27. M. Sato and J. D. Gitlin, *J Biol Chem*, 1991, **266**, 5128-5134.
28. K. H. Schosinsky, H. P. Lehmann and M. F. Beeler, *Clin Chem*, 1974, **20**, 1556-1563.
29. R Development Core Team, *R: A language and environment for statistical computing*, R Foundation for Statistical Computing, 2011.
30. T. Hothorn, F. Bretz and P. Westfall, *Biometrical journal. Biometrische Zeitschrift*, 2008, **50**, 346-363.
31. H. Wickham, *ggplot2: Elegant Graphics for Data Analysis* Springer Publishing Company, Incorporated, 2nd edn., 2009.
32. G. Box and D. Cox, *Journal of the Royal Statistical Society. Series B (Methodological)* 1964, **26**, 211-252
33. J. R. Prohaska, *Advances in nutrition*, 2011, **2**, 89-95.

34. V. N. Zaitsev, I. Zaitseva, M. Papiz and P. F. Lindley, *J Biol Inorg Chem*, 1999, **4**, 579-587.
35. N. E. Hellman and J. D. Gitlin, *Annu Rev Nutr*, 2002, **22**, 439-458.
36. L. W. Gray, T. Z. Kidane, A. Nguyen, S. Akagi, K. Petrasek, Y. L. Chu, A. Cabrera, K. Kantardjieff, A. Z. Mason and M. C. Linder, *Biochem J*, 2009, **419**, 237-245.
37. M. C. Patterson, C. J. Hendriksz, M. Walterfang, F. Sedel, M. T. Vanier, F. Wijburg and N.-C. G. W. Group, *Mol Genet Metab*, 2012, **106**, 330-344.
38. M. C. Patterson, D. Vecchio, H. Prady, L. Abel and J. E. Wraith, *Lancet Neurol*, 2007, **6**, 765-772.
39. C. Lentner, (Ed.), *Geigy Scientific Tables: Units of Measurement, Body Fluids, Composition of the Body, Nutrition*, Ciba-Geigy Corporation Medical Education Division, Basel, Switzerland, 8th edn., 1981.
40. N. M. Yanjanin, J. I. Velez, A. Gropman, K. King, S. E. Bianconi, S. K. Conley, C. C. Brewer, B. Solomon, W. J. Pavan, M. Arcos-Burgos, M. C. Patterson and F. D. Porter, *Am J Med Genet B Neuropsychiatr Genet*, 2010, **153B**, 132-140.
41. C. H. Campbell, R. Brown and M. C. Linder, *Biochim Biophys Acta*, 1981, **678**, 27-38.
42. S. H. Lee, R. Lancey, A. Montaser, N. Madani and M. C. Linder, *Proc Soc Exp Biol Med*, 1993, **203**, 428-439.
43. I. Ribeiro, A. Marcao, O. Amaral, M. C. Sa Miranda, M. T. Vanier and G. Millat, *Hum Genet*, 2001, **109**, 24-32.
44. W. D. Park, J. F. O'Brien, P. A. Lundquist, D. L. Kraft, C. W. Vockley, P. S. Karnes, M. C. Patterson and K. Snow, *Hum Mutat*, 2003, **22**, 313-325.

45. R. Fu, N. M. Yanjanin, M. J. Elrick, C. Ware, A. P. Lieberman and F. D. Porter, *Am J Med Genet A*, 2012, **158A**, 2775-2780.
46. M. Miyata and J. D. Smith, *Nat Genet*, 1996, **14**, 55-61.
47. B. R. Roszell, J. Q. Tao, K. J. Yu, L. Gao, S. Huang, Y. Ning, S. I. Feinstein, C. H. Vite and S. R. Bates, *PLoS ONE*, 2013, **8**, e67084.
48. A. Muralidhar, I. A. Borbon, D. M. Esharif, W. Ke, R. Manacheril, M. Daines and R. P. Erickson, *Mol Genet Metab*, 2011, **103**, 142-147.
49. C. R. Capo, M. Arciello, R. Squitti, E. Cassetta, P. M. Rossini, L. Calabrese and L. Rossi, *Biometals*, 2008, **21**, 367-372.
50. E. L. Que, D. W. Domaille and C. J. Chang, *Chem Rev*, 2008, **108**, 1517-1549.
51. S. M. Cologna, C. V. Cluzeau, N. M. Yanjanin, P. S. Blank, M. K. Dail, S. Siebel, C. L. Toth, C. A. Wassif, A. P. Lieberman and F. D. Porter, *J Inherit Metab Dis*, 2013.
52. S. L. Sensi, P. Paoletti, A. I. Bush and I. Sekler, *Nat Rev Neurosci*, 2009, **10**, 780-791.
53. B. K. Bitanhirwe and M. G. Cunningham, *Synapse*, 2009, **63**, 1029-1049.
54. J. W. Totenhagen, S. Lope-Piedrafita, I. A. Borbon, E. S. Yoshimaru, R. P. Erickson and T. P. Trouard, *J Magn Reson Imaging*, 2012, **35**, 528-536.
55. A. S. Prasad, A. Miale, Jr., Z. Farid, H. H. Sandstead and A. R. Schulert, *J Lab Clin Med*, 1963, **61**, 537-549.
56. H. H. Sandstead, *Advances in nutrition*, 2013, **4**, 76-81.
57. W. L. An, C. Bjorkdahl, R. Liu, R. F. Cowburn, B. Winblad and J. J. Pei, *J Neurochem*, 2005, **92**, 1104-1115.
58. Z. Y. Mo, Y. Z. Zhu, H. L. Zhu, J. B. Fan, J. Chen and Y. Liang, *J Biol Chem*, 2009, **284**, 34648-34657.

59. I. A. Auer, M. L. Schmidt, V. M. Lee, B. Curry, K. Suzuki, R. W. Shin, P. G. Pentchev, E. D. Carstea and J. Q. Trojanowski, *Acta Neuropathol*, 1995, **90**, 547-551.
60. N. Sawamura, J. S. Gong, W. S. Garver, R. A. Heidenreich, H. Ninomiya, K. Ohno, K. Yanagisawa and M. Michikawa, *J Biol Chem*, 2001, **276**, 10314-10319.
61. S. Treiber-Held, R. Distl, V. Meske, F. Albert and T. G. Ohm, *J Pathol*, 2003, **200**, 95-103.
62. R. Distl, V. Meske and T. G. Ohm, *Acta Neuropathol*, 2001, **101**, 547-554.
63. T. J. Craddock, J. A. Tuszynski, D. Chopra, N. Casey, L. E. Goldstein, S. R. Hameroff and R. E. Tanzi, *PLoS ONE*, 2012, **7**, e33552.
64. K. M. Kanninen, A. Grubman, A. Caragounis, C. Duncan, S. J. Parker, G. E. Lidgerwood, I. Volitakis, G. Ganio, P. J. Crouch and A. R. White, *Biology open*, 2013, **2**, 635-646.
65. K. M. Kanninen, A. Grubman, J. Meyerowitz, C. Duncan, J. L. Tan, S. J. Parker, P. J. Crouch, B. M. Paterson, J. L. Hickey, P. S. Donnelly, I. Volitakis, I. Tammen, D. N. Palmer and A. R. White, *PLoS ONE*, 2013, **8**, e58644.
66. A. Terman and T. Kurz, *Antioxid Redox Signal*, 2013, **18**, 888-898.

## Figure legends

**Figure 1** Altered metal homeostasis in the *Npc1*<sup>-/-</sup> mouse model. Major organ tissues were collected from P49 female *Npc1*<sup>-/-</sup> and wild-type (WT) littermate control mice (n = 14/genotype). Mn, Fe, Cu, and Zn concentrations were significantly changed in selected *Npc1*<sup>-/-</sup> tissues (cerebellum, cerebrum, and liver) compared to WT. See Table S1 for detailed metal analysis of major organs from the *Npc1*<sup>-/-</sup> mouse model. Metal levels were determined by ICP-MS. Data represent mean ± S.E.M. Statistical analysis: Student's *t*-test. \*\**p* < 0.01; \*\*\**p* < 0.001.

**Figure 2** Altered plasma metal and CP homeostasis in the *Npc1*<sup>-/-</sup> mouse model. Heparinized plasma samples were collected from P21 (n = 5/genotype) and P49 (n = 18/genotype) female *Npc1*<sup>-/-</sup> and wild-type (WT) littermate control mice. Significant changes in *Npc1*<sup>-/-</sup> plasma (A) Mn, (B) Fe, (C) Cu and (D) Zn concentrations; (E) total CP levels; (F) total oxidase activity; (G) apo- and holo-CP levels; and (H) CP and azide-resistant oxidase activity levels were age- and disease-dependent. Metal levels were determined by ICP-MS. Total, holo- and apo-CP levels were measured by western blotting (see Figure S1). Total, CP and azide-resistant oxidase activities were determined by the *o*-dianisidine oxidase assay. CP oxidase activity was calculated as the difference between total and azide-resistant oxidase activities. Data represent mean ± S.E.M. Statistical analysis: Two-way ANOVA with Bonferroni correction for multiple comparisons. \**p* ≤ 0.05; \*\**p* ≤ 0.01; \*\*\**p* ≤ 0.001.

**Figure 3 Zinc accumulates in human NP-C cerebellum.** Metal analysis of human post-mortem cerebellar (n = 4/group) and hippocampal (n = 5/group) tissues from NP-C and age- and gender-matched non-NP-C control subjects. Metal concentrations in cerebellar and hippocampal tissues were measured by ICP-MS and normalized to tissue wet weight. Data represent mean  $\pm$  S.E.M. Statistical analysis: Student's *t*-test. \* $p \leq 0.05$ .

**Figure 4 Human NP-C1 CSF is deficient in transition metals.** Scatterplots of CSF (A) Mn, (B) Fe, (C) Cu, and (D) Zn concentrations in human NP-C1 cases (n = 21). The majority of the NP-C1 cases have CSF (B) Fe, (C) Cu and (D) Zn concentrations below their respective reference range (dashed lines), independent of age, disease severity, gender and miglustat treatment. Metal concentrations were measured by ICP-MS. Data represent mean  $\pm$  S.D. [Reference range: Lentner, C., (Ed.) (1981) *Geigy Scientific Tables: Units of Measurement, Body Fluids, Composition of the Body, Nutrition*. Ciba-Geigy Corporation Medical Education Division, Basel, Switzerland.]

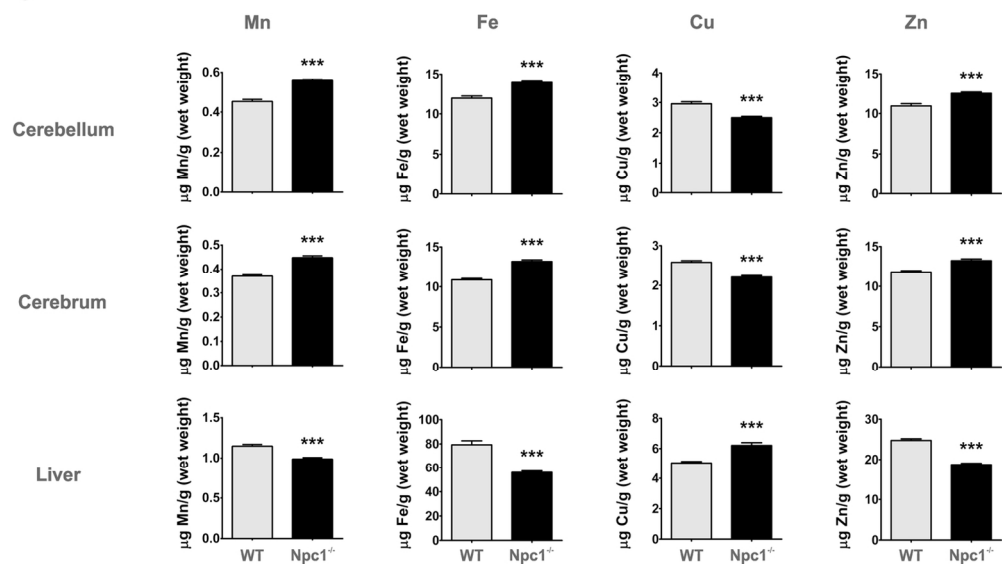
**Figure 5 Changes in NP-C1 CSF CP and metal homeostasis.** (A) A moderate, but significant positive correlation between NP-C disease severity with CSF total and holo-CP concentrations. (B) There was a significant negative correlation between NP-C1 CSF Cu and apo-CP. (C) The CSF Mn concentration was significantly associated with both total and holo-CP levels. CSF total, holo- and apo-CP concentrations were measured using purified human CP standards and western blotting (see Figure S2A). Statistical analysis: multiple linear regression was performed, adjusting for age and gender (n = 21). Shaded areas denote 95% confidence interval.

**Figure 6** **Altered plasma Mn, Fe and Zn homeostasis in NP-C1 patients.** Metal analysis of heparinized plasma samples from NP-C1 cases (n = 40) and age-matched healthy controls (HC; n = 41). There was a significant decrease in (A) Mn, (B) Fe and (C) Zn in the NP-C1 plasma samples compared to HC. The frequency of NP-C1 patients (12%) with plasma zinc below the reference range is significantly greater than HC (5%; p = 0.04). These changes were not affected by miglustat treatment. Metal concentrations were measured by ICP-MS. Box and whiskers plot depict the median, the inter-quartile range (IQR), and the highest and lowest values within 1.5 times the IQR. Statistical analysis: ANCOVA followed by multiple pairwise comparison using the Tukey contrasts with false discovery correction. \*p ≤ 0.05; \*\*p ≤ 0.01; \*\*\*p ≤ 0.001. [Reference range (dashed lines): Tietz, N.W. (1987). *Fundamentals of clinical chemistry*, 3rd edn. Saunders, Philadelphia. P: pediatric (≤ 21 years old); ♀: female; ♂: male.]

**Figure 7** **Miglustat alters human NP-C1 patient plasma CP homeostasis.** There were no significant differences in the mean plasma (A) total and (C) apo-CP concentrations between non-NP-C healthy controls (HC; n = 41) and NP-C1 cases not treated (n = 16) and treated with miglustat (n = 24). However, (B) plasma holo-CP was significantly increased by 17% in NP-C1 patients treated with miglustat. Despite an increase in holo-CP, NP-C1 patients treated with miglustat had significantly lower (D) Cu:total CP and (E) Cu:holo-CP ratios compared to HC and NP-C1 patients not treated with miglustat. (F) This was reflected in a significantly reduced holo-CP specific activity in NP-C1 patients treated with miglustat compared to those not treated with miglustat. (G) Plasma apo-CP in NP-C1 patients was significantly associated with disease severity, and this was gender-dependent, but independent of miglustat treatment (p = 0.016). Plasma total, holo- and apo-CP concentrations were measured using purified human CP

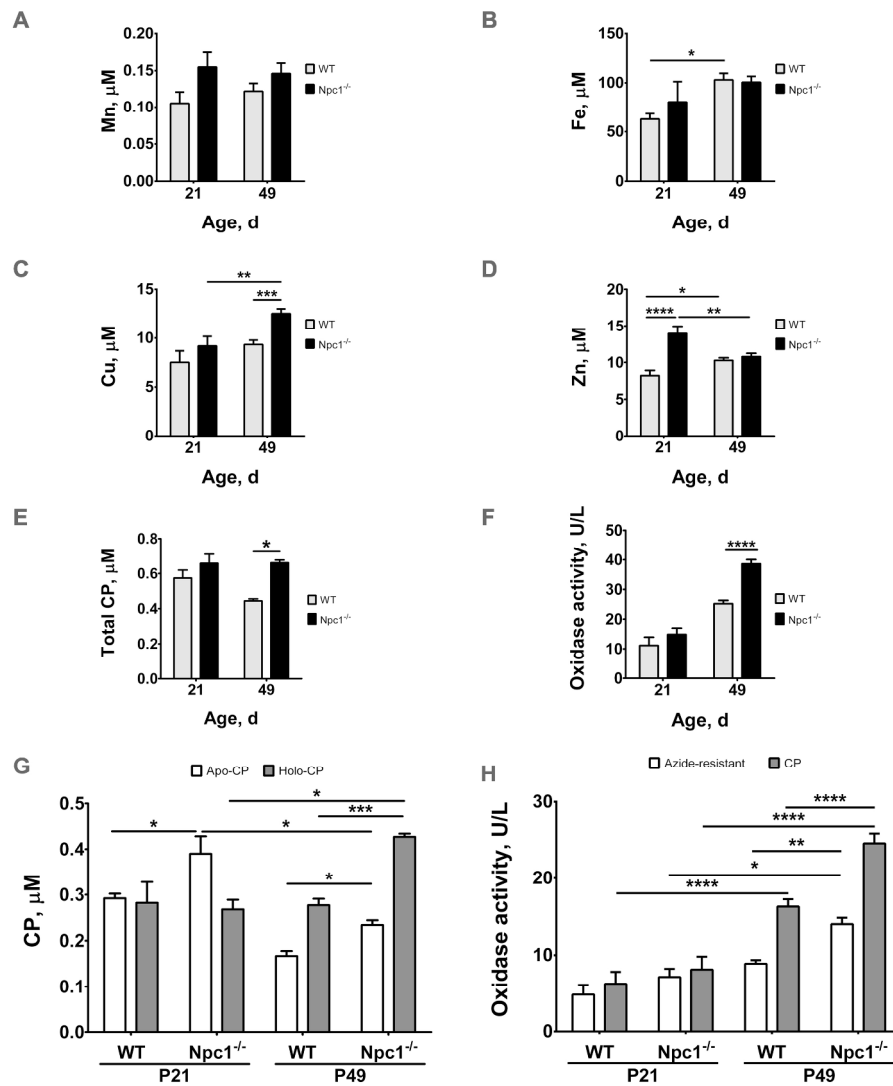
standards and western blotting (see Figure S2B). Box and whiskers plot depict the median, the inter-quartile range (IQR), and the highest and lowest values within 1.5 times the IQR. Statistical analysis: (A – F) ANCOVA followed by multiple pairwise comparison using the Tukey contrasts with false discovery correction; (G) multiple linear regression was performed, adjusting for age, gender and miglustat status.  $*p \leq 0.05$ ;  $**p \leq 0.01$ . Shaded areas denote 95% confidence interval.

Figure 1



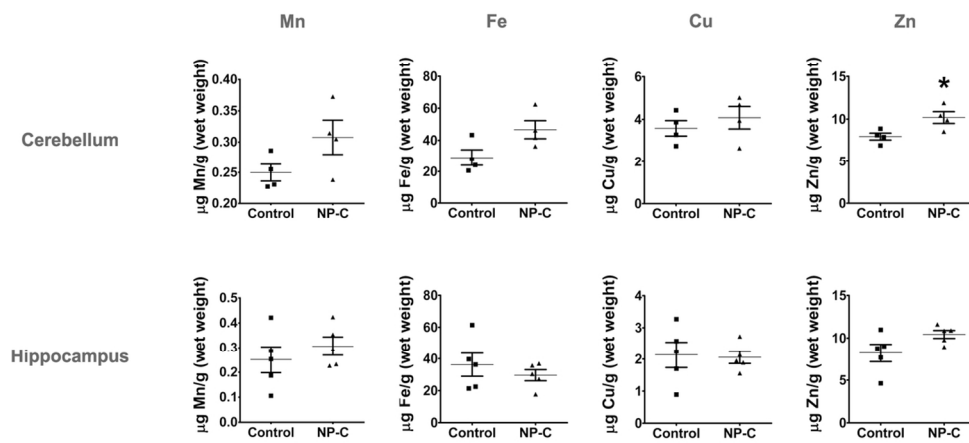
130x75mm (300 x 300 DPI)

Figure 2



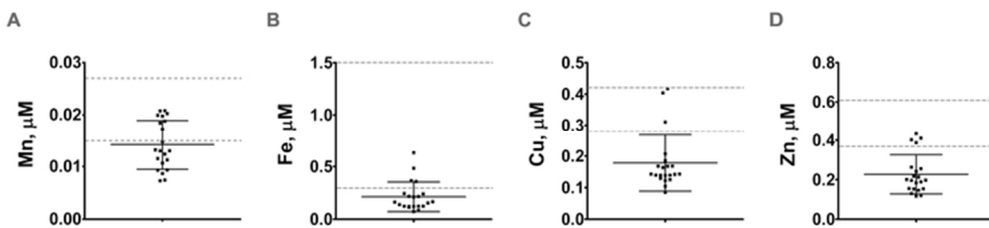
226x285mm (300 x 300 DPI)

Figure 3



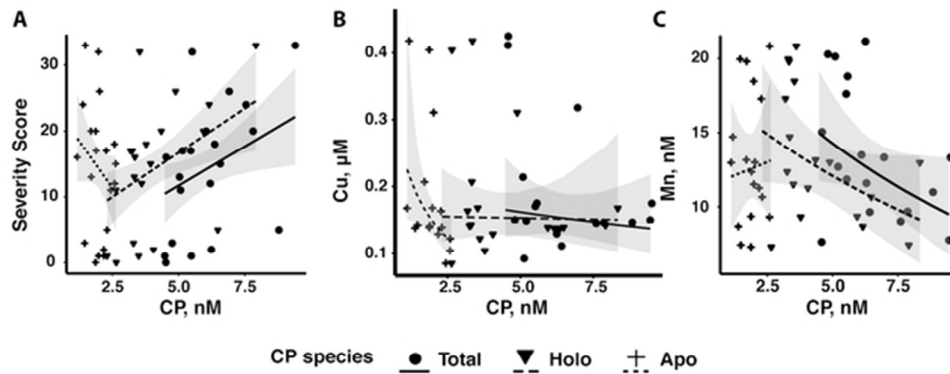
113x54mm (300 x 300 DPI)

Figure 4



64x18mm (300 x 300 DPI)

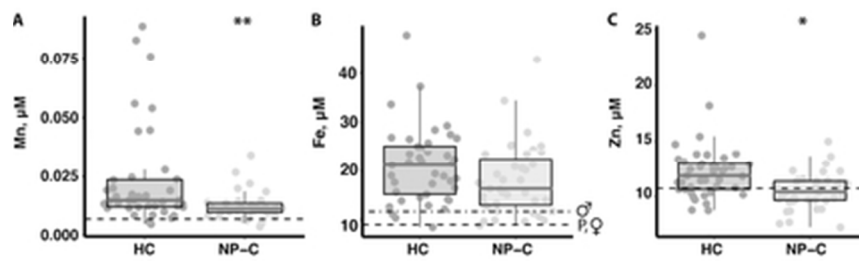
Figure 5



	Partial R <sup>2</sup>	<i>p</i>	Partial R <sup>2</sup>	<i>p</i>	Partial R <sup>2</sup>	<i>p</i>
Total CP	0.110	<b>0.026</b>	0.029	0.512	0.35	<b>0.009</b>
Holo-CP	0.147	<b>0.007</b>	0.0006	0.924	0.369	<b>0.008</b>
Apo-CP	0.056	0.148	0.216	<b>0.034</b>	0.006	0.771

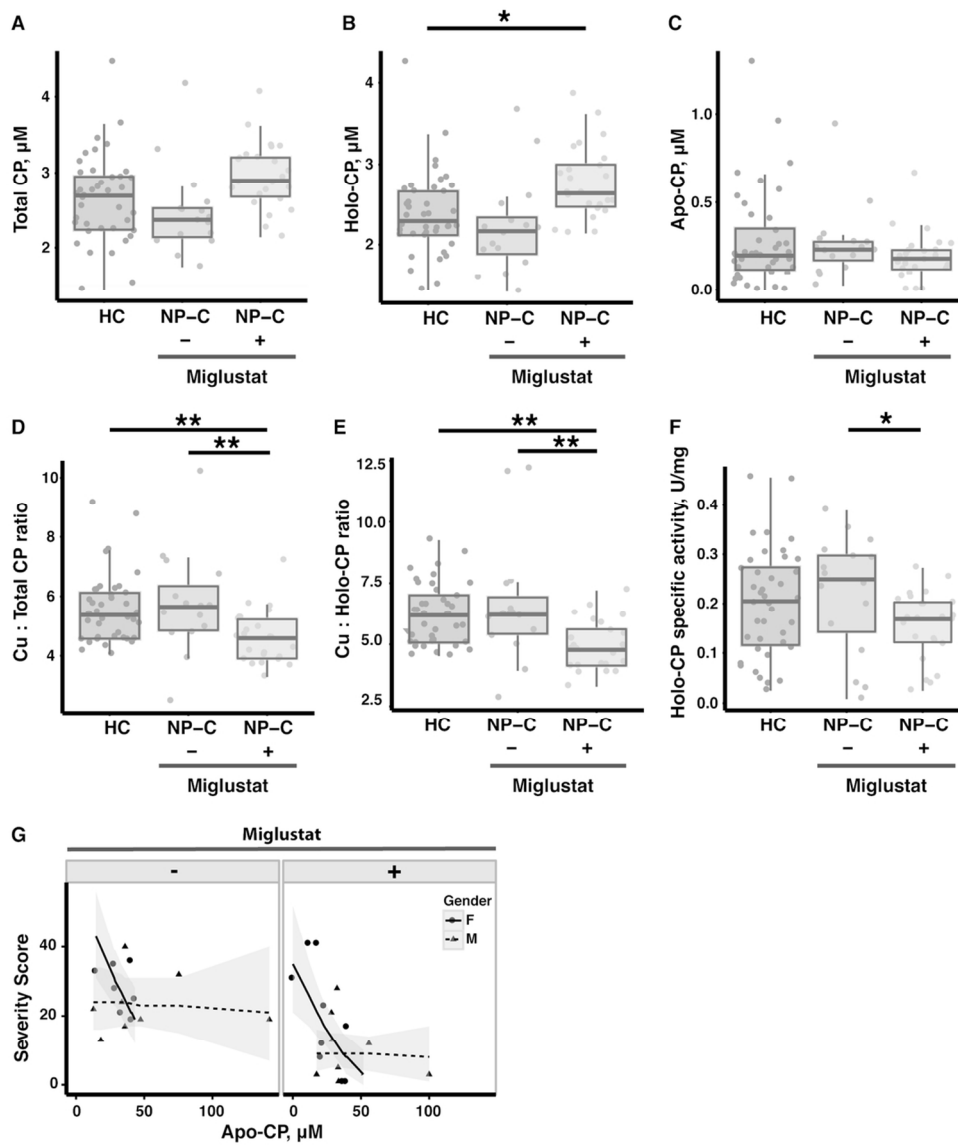
56x34mm (300 x 300 DPI)

Figure 6



36x12mm (300 x 300 DPI)

Figure 7



103x121mm (300 x 300 DPI)